



Title	Smart Transformer and Low Frequency Transformer Comparison on Power Delivery Characteristics in the Power System
Authors(s)	Chen, Junru, Zhu, Rongwu, O'Donnell, Terence, Liserre, Marco
Publication date	2018-10-05
Publication information	Chen, Junru, Rongwu Zhu, Terence O'Donnell, and Marco Liserre. "Smart Transformer and Low Frequency Transformer Comparison on Power Delivery Characteristics in the Power System." IEEE, October 5, 2018. https://doi.org/10.23919/aeit.2018.8577375 .
Conference details	AEIT 2018 International Annual Conference, Bari, Italy, 3-5 October 2018
Publisher	IEEE
Item record/more information	http://hdl.handle.net/10197/10566
Publisher's statement	Authors/employers retain all proprietary rights in any process, procedure, or article of manufacture described in the Work. Authors/employers may reproduce or authorize others to reproduce the Work, material extracted verbatim from the Work, or derivative works for the author's personal use or for company use, provided that the source and the AEIT copyright notice are indicated, the copies are not used in any way that implies AEIT endorsement of a product or service of any employer, and the copies themselves are not offered for sale. Although authors are permitted to re-use all or portions of the Work in other works, this does not include granting third-party requests for reprinting, republishing, or other types of re-use. AEIT must handle all such third-party requests.
Publisher's version (DOI)	10.23919/aeit.2018.8577375

Downloaded 2026-05-01 23:37:43

The UCD community has made this article openly available. Please share how this access benefits you. Your story matters! (@ucd_oa)



© Some rights reserved. For more information

Smart Transformer and Low Frequency Transformer Comparison on Power Delivery Characteristics in the Power System

Junru Chen¹, Rongwu Zhu², Terence O'Donnell¹, Marco Liserre²

1. University College Dublin, Dublin, Ireland

2. Chair of Power Electronics, Christian-Albrechts-Universität zu Kiel, Kiel, Germany
Junru.chen.1@ucdconnect.ie

Abstract—Smart transformer is a power electronics-based transformer, offering voltage regulation and DC connectivity. As a transformer, its basic function is still power delivery. Smart transformer with advanced controls can support MV grid voltage by absorbing/injecting reactive power while actively regulate the LV grid voltage. Due to the controllable voltage in both MV and LV side, the power delivery of smart transformer is flexible. This paper focuses on the power delivery characteristic of smart transformer and compares with the conventional low frequency transformer with the help of STATCOM at its primary side or on load tap changer at its secondary side, in the power system by means of maximum deliverable power and power-voltage curve analysis. The Simulink results validate that the smart transformer improves system voltage stability compared to the traditional low frequency transformer with load tap changer.

Keywords—smart transformer, low frequency transformer, power delivery, voltage stability

I. INTRODUCTION

The increasing penetration of distribution generator (DG) and electric vehicle (EV) requires the improvement of flexibility in the power system. Smart transformer (ST), a power electronics-based transformer, can provide connectivity to DC network [1] and reduce the infrastructure cost caused by the needed reinforcements of the lines due to DG and EV charging station. Moreover, the ST can provide such flexibility on hybrid AC/DC grids operation and voltage support [1].

Voltage instability results from the attempt of loads to draw more power than can be delivered by the transmission and generation system. Low frequency transformer (LFT) has been widely used for the power delivery in current network. However, LFT consists of coils and magnetic core, absorbing reactive power for magnetizing, degrading the maximum deliverable power and may give rise to voltage stability problems.

To address voltage issues, STATCOM can be co-located with the LFT to support the voltage in the primary side by compensating reactive power, and on the other hand a on-load tap changer (OLTC) is implemented into LFT to vary the voltage on the secondary side according to the load in order to operate the system with large electrical distances between generators and loads. These actions obviously requires more space for LFT and increase the costs. In contrast, ST is a more economical way to achieve the voltage compensation in primary side and voltage regulation in secondary side without the need of the STATCOM and OLTC [3].

ST is a power electronics-based transformer with merits of not only small size and weight, but also the isolation of reactive

power for each terminal, which avoids the LVAC side absorbing reactive power from MVAC grid and consequently avoids corresponding effects from LVAC grid on MVAC grid for direct voltage reduction as the conventional LFT. Moreover, due to the advanced control functionalities, ST can compensate the reactive power in order to support the MVAC grid voltage, behaved as the conventional STATCOM [4], and on the other side, the voltage and frequency in the LVAC side can be fully controlled by the ST, which gives the possibility to control the demand as OLTC does [5] but with fast dynamic. Therefore, the power delivery of ST is more flexible and robust.

The contribution of this paper is to mathematically analyse the power delivery characteristics of ST and compare with traditional LFT combined with the STATCOM on its primary side or OLTC on its secondary side. The power delivery characteristic discussed in the paper includes maximum deliverable power and power-voltage curve, both of which are related to the voltage stability.

The paper is organized as follows: Section II introduces the computation of power delivery between two-bus infinite system. Section III reviews the power delivery of LFT with and without STATCOM or OLTC. Section IV analyses the power delivery of ST. Section V studies the cases to compare ST to LFT with OLTC in terms of power delivery and voltage stability. Finally, Section VI draws the conclusions.

II. POWER DELIVERY

Power delivery characteristic can be studied by an infinite-bus system as shown in Fig. 1. The source side voltage is constant and determined by generator voltage, so that the power flow interacts to the receiving-end voltage. This section explains this interaction by the mathematical analysis.

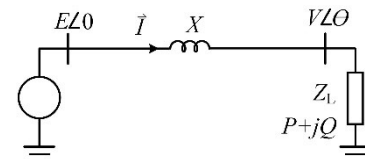


Fig.1 Single-load infinite-bus system

A. Maximum Deliverable Power

In Fig. 1, the system consists of a load Z_L consuming active power P and reactive power Q under voltage V fed by an infinite bus, E , through a lossless transmission line with inductance X [6,7]. Specifying that the load power factor is $\cos\varphi$ and the load impedance is $Z_L = R_L + jR_L \tan\varphi$, where R_L is the load resistance. From Fig. 1, the current \vec{I} can be computed as:

$$\vec{I} = \frac{E}{R_L + j(X + R_L \tan\varphi)} \quad (1)$$

The load active power is:

$$P = R_L I^2 = \frac{R_L E^2}{R_L^2 + (X + R_L \tan\varphi)^2} \quad (2)$$

When the derivative of load active power to the load impedance is zero ($\partial P / \partial R_L = 0$), the extremum condition for maximum power can be obtained as,

$$X^2 = R_L^2 (1 + \tan^2\varphi) \quad (3)$$

Then the load impedance under such situation is $R_{L,Pmax} = X \cos\varphi$. By substituting $R_{L,Pmax}$ into (2), it yields the maximum active power (4) and corresponding voltage (5).

$$P_{max} = \frac{\cos\varphi}{1 + \sin\varphi} \cdot \frac{E^2}{2X} \quad (4)$$

$$V_{Pmax} = \frac{E}{\sqrt{2}\sqrt{1 + \sin\varphi}} \quad (5)$$

Therefore, in a certain line, the maximum possible loading is determined by (4) with the voltage (5). From (4) and (5), the leading power factor increases the maximum loading and its corresponding load voltage, while the lagging power factor reduces the maximum loading and its voltage. Thus, the reactive power compensation can improve the voltage stability and extend the maximum loading.

B. Power-voltage Curve

The maximum deliverable power is the extremum case for the power delivery. Normally, the load active power is far below its maximum value, and its voltage is constrained on the (1 ± 0.1) pu or (1 ± 0.05) pu by different grid codes.

Still based on Fig. 1, the load voltage is $\vec{V} = E - jX\vec{I}$, and the load complex power is expressed as,

$$\begin{cases} P + jQ = \vec{V} \cdot \vec{I}^* \\ \begin{cases} P = -\frac{EV}{X} \sin\theta \\ Q = -\frac{V^2}{X} + \frac{EV}{X} \cos\theta \end{cases} \end{cases} \quad (6)$$

By eliminating θ in (6), the relationship among the power and voltage can be obtain as,

$$V = \sqrt{\frac{E^2}{2} - QX} \pm \sqrt{\frac{E^4}{4} - P^2 X^2 - QXE^2} \quad (7)$$

Based on (7), the power-voltage curve is shown in Fig. 2. When the sign of $\sqrt{E^4/4 - P^2 X^2 - QXE^2}$ is plus, the voltage locates the stable operating area (solid blue line) while minus sign leading to the unstable operating area (dotted blue line). For a load, P_L , there are two crossing points with voltage-power curve, A and B, but only point A is stable. The maximum point (P_{max}, V_{Pmax}) is the Saddle-node bifurcation (SNB) point.

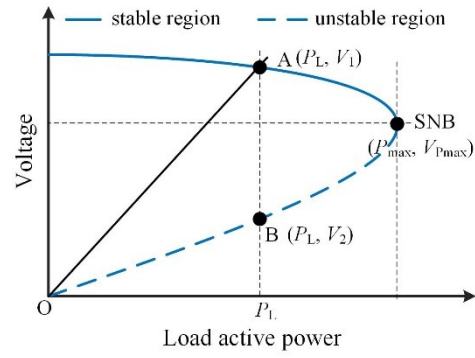


Fig.2 Power-voltage curve

C. Load Curve

In reality, the load is not independent of the operating voltage, and a static exponential model [8] is widely used,

$$P = P_0 \left(\frac{V}{V_0}\right)^\alpha \quad (8)$$

where P_0 is the nominal power at the nominal voltage V_0 and α is the load voltage sensitivity. When $\alpha = 0$, the load is a constant power load and its curve is line AB, and when $\alpha = 1$, the load curve is line OA as shown in Fig. 2.

III. LOW FREQUENCY TRANSFORMER

In previous, only a simplified system without LFT is considered, while LFTs are widely used in power networks. Therefore, the impact of LFT on power delivery is studied. Moreover, the power delivery characteristic of LFT with the support of STATCOM and OLTC is analysed as well.

A. Effects of LFT

The inclusion of LFT breaks the line impedance X in Fig. 1 into two part X_1 and X_2 , which are the primary and secondary side transmission line impedance, respectively. In the study the LFT is modeled considering its short-circuit reactance X_t [6,7], by adding its leakage reactance X_t to the secondary side or load side, as shown in Fig. 3. Note, in per unit frame, $X_1 + X_2 = X$.

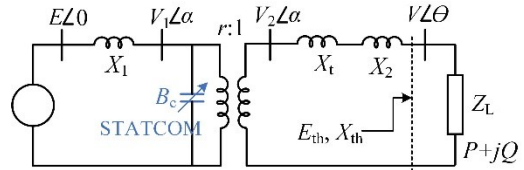


Fig. 3. Single-load infinite-bus system with LFT

Since transform ratio r is 1 in per unit, $V_1 = V_2$ in Fig. 3. In comparison with Fig. 1, the only difference is the line impedance increased by transformer leakage reactance X_t . Consequently, if replacing X with $X + X_t$ in (4) and (5), the maximum deliverable power and its load voltage can be expressed as (9) and (10).

$$P_{max} = \frac{\cos\varphi}{1 + \sin\varphi} \cdot \frac{E^2}{2(X + X_t)} \quad (9)$$

$$V_{Pmax} = \frac{1}{1 - (X + X_t)} \cdot \frac{E}{\sqrt{2}\sqrt{1 + \sin\varphi}} \quad (10)$$

Compared to no LFT case, the maximum deliverable power is reduced and the power-voltage curve can be plotted as red line in Fig. 3. Under the same loading condition, P_{L1} , the stable operating point moves from A to B, leading to operating voltage reduced and then the system stability degraded.

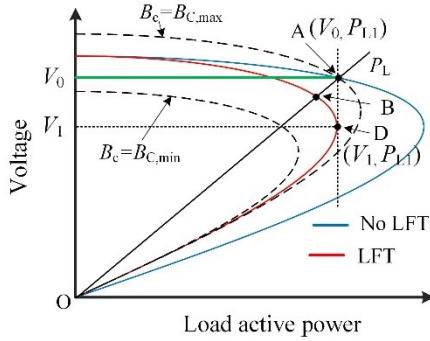


Fig. 4 Power-voltage curve comparison of no LFT, with LFT and with LFT+STATCOM

B. LFT combed with STATCOM

STATCOM is a typical way to solve the power capacity reduction and voltage stability degradation, which is based on a power converter and can act as either a source or sink of reactive power in network. It is used to compensate the reactive power and further enhance the system voltage stability. STATCOM can be either co-located to the LFT [9] or not. If co-located to the LFT, the interaction between LFT and STATCOM increases the system harmonics [10] and makes the transient current in STATCOM surge after faults [11]. An optimal location for STATCOM in network was proposed in [12]. The model of STATCOM can be equivalent as a controllable capacitor B_c paralleling on bus V_i in Fig. 3, where B_c is constrained by STATCOM equivalent capacitor $B_{c,min} \leq B_c \leq B_{c,max}$, which is regulated as a voltage droop with gain K ,

$$B_c = K(V_0 - V) \quad (11)$$

Then the corresponding compensation reactive power is:

$$Q_c = B_c \cdot V_1^2 \quad (12)$$

The Thevenin equivalent as seen by the load (the left part of the dashed line in Fig. 3) has following emf and reactance:

$$\begin{cases} E_{th} = \frac{E}{1 - B_c X_1} \\ X_{th} = \frac{X_1}{1 - B_c X_1} + X_2 + X_t \end{cases} \quad (13)$$

Substituting (13) into (4) and (5) could obtain the maximum deliverable power and its corresponding voltage.

$$P_{max} = \frac{\cos\varphi}{1 + \sin\varphi} \cdot \frac{E^2}{2(X + X_t) - 2B_c X_1(X_2 + X_t)} \quad (14)$$

$$V_{Pmax} = \frac{1}{1 - B_c(X + X_t)} \cdot \frac{E}{\sqrt{2}\sqrt{1 + \sin\varphi}} \quad (15)$$

Compared with no STATCOM case (9) and (10), STATCOM can increase the maximum power delivery and its operating voltage.

Substituted (13) into (7), the power-voltage curve, effected by B_c , is varied within two boundary lines (dotted black lines) where B_c is equalling to $B_{c,min}$ and $B_{c,max}$, respectively, as shown in Fig. 4. Due to the flexible operation ranges of power-voltage curve, STATCOM can keep the operating voltage constant and thus operating trajectory is changed from the line OA to be constant value of V_0 , as shown by the green line. It also depicts that with the help of STATCOM, the operating point can recover from B to A.

C. LFT combed with OLTC

Another method to support load voltage is OLTC, by varing the turn ratio r in a discrete step. When the load voltage below the nominal value, r will be reduced to increase the secondary voltage, while the primary voltage remains. In this case, the line from generator to load is broken to generator to the primary side of LFT and secondary side of LFT to load. For the load, the LFT now can be regarded as an isolated supply or sending terminal, and thus it can help shorten the electric distance. Compared to the STATCOM, which is a receiving-end voltage supporter, OLTC is a sending-end voltage supporter. Because OLTC is a mechanism, it needs a certain time for one step shift, normally 5s and each step shift is discrete. Hence, it is a slow regulation. The dynamic loads may cause the OLTC oscillation so that the threshold is required. Moreover, in multiple OLTC levels, the coordination between upper OLTC and lower OLTC needs to be strictly scheduled, otherwise, their interaction will trap both taps oscillating [5]. The model of LFT combined with OLTC can be equivalent as LFT with a variable r . Similar to (13), the Thevenin equivalent is obtained,

$$\begin{cases} E_{th} = \frac{E}{r} \\ X_{th} = \frac{X_1}{r^2} + X_2 + X_t \end{cases} \quad (16)$$

Substituting (16) into (4) and (5) could obtain the maximum deliverable power and its corresponding voltage.

$$P_{max} = \frac{\cos\varphi}{1 + \sin\varphi} \cdot \frac{E^2}{2(X_1 + r^2 X_2 + r^2 X_t)} \quad (17)$$

$$V_{Pmax} = \frac{E}{r\sqrt{2}\sqrt{1 + \sin\varphi}} \quad (18)$$

Compared to (9), no OLTC case ($r=1$), the reduction of ratio can increase the maximum deliverable power and its corresponding voltage.

Due to the LFT, the operating point changes from A to B, but the OLTC can bring the secondary side voltage from B to A, in steady state, as shown in Fig. 4, and thus the load power at the primary and secondary side is both P_{L1} . However, in contrast, operating point of the primary side is D, with voltage V_1 and power P_{L1} , potentially leading to voltage instable.

IV. SMART TRANSFORMER

The basic configuration of a 3-stage ST consisting of AC/DC rectifier, DC/DC converter with high/medium frequency transformer and DC/AC inverter, as shown in Fig.5. The MV AC/DC converter regulates the MVDC voltage; the DC/DC converter controls the LVDC voltage and the LV AC/DC

converter controls LVAC grid voltage with rated frequency and amplitude. Moreover, LVAC load can be dynamically regulated by ST to optimize the losses [13], to achieve minimum demand [14] and to provide upper system frequency support [15].

On another hand, ST only delivers active power in each stage while the reactive power is decoupled. This gives the freedom to the MV AC/DC converter to compensate the reactive power in MVAC side in order to support the voltage, similar to the STATCOM co-located LFT, but without the STATCOM and LFT interaction problems. The voltage in MVAC side and LVAC side is fully decoupled, thus, ST also helps to break the electric distance as the LFT combined with OLTC. With this special structure and its active controls, the power delivery in ST is more flexible and voltage stability is ideally better.

A. LVAC side

With a proper design, ST LVAC voltage precisely tracks its reference, independently to the output impedance. Therefore, unlike LFT, which has output leakage impedance X_t as shown in Fig. 3 and couples to the voltage output V_2 , ST can be seen as a controlled voltage source V_2 directly connected to load through the line impedance X_2 as shown in Fig. 5. P_{DC} represents the power generated by the DC connected renewable energy sources.

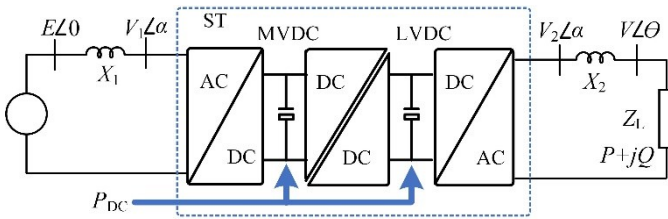


Fig. 5 Single-load infinite-bus system with ST

In LVAC side, the ST output voltage is V_2 and the line impedance between ST and load is X_2 , which is smaller than the impedance in LFT with OLTC case, increasing power delivery capability. Replacing E with V_2 and X with X_2 could obtain the maximum deliverable power in ST-LVAC system.

$$P_{max} = \frac{\cos\phi}{1 + \sin\phi} \cdot \frac{V_2^2}{2X_2} \quad (19)$$

$$V_{Pmax} = \frac{V_2}{\sqrt{2}\sqrt{1 + \sin\phi}} \quad (20)$$

The ST output voltage V_2 is controllable in the range of 0.9-1.1pu. Therefore, substituting $E=V_2$ and $X=X_2$ could obtain the power-voltage curve as shown in Fig. 6, where the solid blue line is the nominal case while the dotted blue lines are the operation upper and lower boundary with respect of voltage range 0.9-1.1pu.

Compared (19) to (17), the maximum deliverable power is increased, which gives the flexibility to the total power system. On the other hand, due to the limit of power semiconductors, the ST has strictly overload constrain, which behaves like a constant current load (the red line), determining the normal operation range within the area of "ABCD", as shown in Fig. 6.

B. MVAC side

In the MVAC side, the ST can be equivalent as a AC/DC converter connected to a constant load. Meanwhile, besides transferring the active power, it behaves as a STATCOM to

support MVAC voltage by reactive power regulation. The difference is STATCOM has fixed limits on reactive power

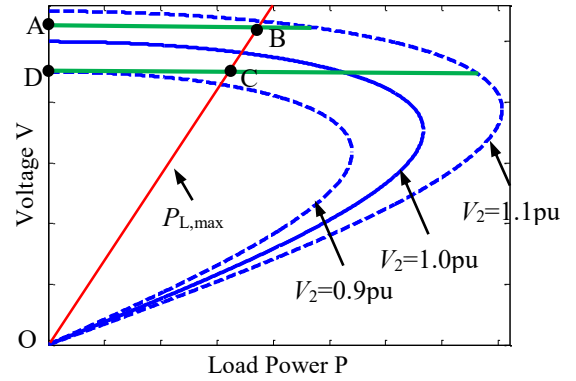


Fig. 6. ST LVAC side power-voltage curve

compensation, i.e. $B_{C,min} \leq B_C \leq B_{C,max}$, while because the main function of ST is transfer active power, the available reactive power is the remaining margin of converter capacity S_{MVAC} after the active power flow ($P - P_{DC}$). The maximum reactive power compensation Q_{max} is given in (21) and the maximum capacitance $B_{C,max}$ is (22).

$$Q_{max} = \sqrt{S_{MVAC}^2 - (P - P_{DC})^2} \quad (21)$$

$$B_{C,max} = \pm Q_{max}/V_1^2 \quad (22)$$

Replacing B_C with $B_{C,max}$ and $X + X_t$ with X_1 in (13) can obtain the Thevenin equivalent as seen by the ST.

$$\begin{cases} E_{th} = \frac{E}{1 \pm X_1 \sqrt{S_{MVAC}^2 - (P - P_{DC})^2}/V_1^2} \\ X_{th} = \frac{X}{1 \pm X_1 \sqrt{S_{MVAC}^2 - (P - P_{DC})^2}/V_1^2} \end{cases} \quad (23)$$

Substituting (23) into (4) and (5) can obtain the maximum deliverable power in ST MVAC side.

$$P_{max} = \frac{1}{1 \pm B_{C,max}X_1} \cdot \frac{\cos\phi}{1 + \sin\phi} \cdot \frac{E^2}{2X_1} \quad (24)$$

$$V_{Pmax} = \frac{1}{1 \pm B_{C,max}X_1} \cdot \frac{E}{\sqrt{2}\sqrt{1 + \sin\phi}} \quad (25)$$

From (23), the voltage support is constrained by the converter capacity S_{MVAC} and loading ($P - P_{DC}$), where is strong in lower loading and weak in higher loading. The maximum deliverable power is increased on the lower loading condition. Moreover, the support capacity can be optimized by designing a proper S_{MVAC} . Moreover, the support capacity can be optimized by designing a proper S_{MVAC} .

Substituting (23) into (7) can obtain the power voltage curve and its voltage support range (dotted red line in Fig. 7). Still the red line ob is the maximum converter loading. It can be seen that in the maximum converter loading point b, there is no space for the voltage variation, due to the disabled reactive power

compensation. The dotted blue lines are the bound of the possible operation curve corresponding to the maximum reactive compensation. The normal operating area is “abc” as shown in Fig. 7. The load to MVAC converter is constant as shown in dotted black line. Without reactive power compensation, the operating point is located in A, while with ST voltage support, it can move along the line BC.

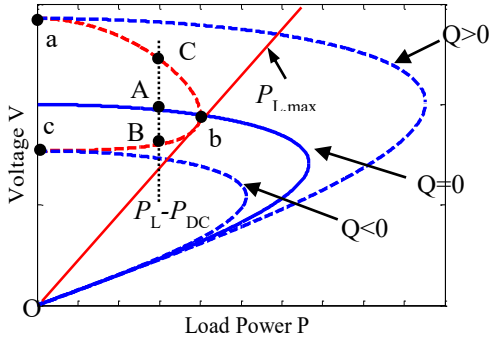


Fig. 7 ST MVAC side Power-voltage curve

C. Smart transformer operation

From aforementioned analysis, the ST operation firstly determines the LVAC side voltage considering the load performance line OB in Fig. 6. This could obtain the loading P_L and then subtracting the generated DC power P_{DC} could obtain the load line BC in Fig. 7. Then the MVAC side voltage can be varied to increase the maximum deliverable power. Therefore, compared with the LFT, ST has more flexible on power delivery and further improves the system voltage stability.

V. CASE STUDY

Since the power delivery characteristic is different between the LFT combined with OLTC and ST, the case study compares their performance after contingency by means of a two-bus system (Fig. 3 and Fig. 5) simulated in Matlab/Simulink and then analyses their operation by means of power-voltage curves. The demo of “power_OLTCregtransformer” in Matlab Sample Library is used directly by scaling to 25kV in primary and 10kV in secondary side, respectively. To speed up the simulation, the time constant of tap selection is reduced from 5s to 1.5s and the ST is simplified as a back-to-back converter. The OLTC transformer is replaced by a ST for the ST case study with the parameters summarized in Table I. The contingency happened at 5s where the grid voltage E is stepped down from 1 to 0.9pu. The results of LVAC and MVAC voltage, and active and reactive power in MVAC bus are shown in Fig. 8.

TABLE I
SIMULATION PARAMETERS

Parameters	Value	Parameters	Value
MV-LVAC voltage(kV)	25-10	Frequency (Hz)	60
MV line resistance (Ω)	0.063	LV line resistance (Ω)	1.153
MV line inductance (Ω)	j0.625	LV line inductance (Ω)	j1.979
ST DC voltage (kV)	20	ST capacity (MVA)	50
ST filter inductance in LV side (mH)	0.85	ST filter inductance in MV side (mH)	5.3
ST filter capacitance in LV side (mF)	1.6	Resistive load (MW)	36

Initially, both MV and LV side voltage is regulated to the nominal value, 1.0pu, in 4-5s, for both cases of LFT+OLTC and

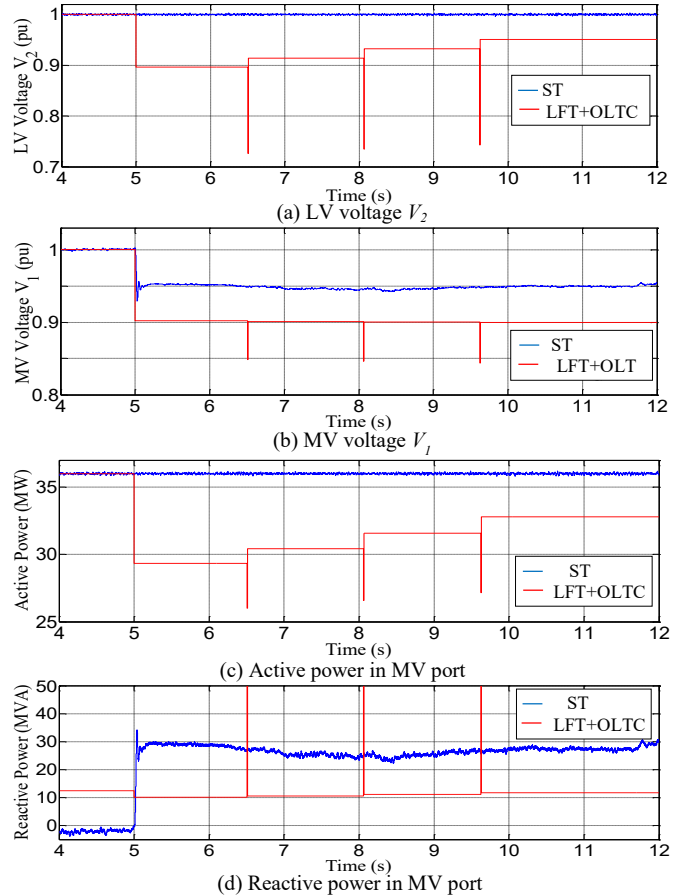


Fig. 8. Case study results comparison of ST with LFT+OLTC

ST, as shown in Fig. 8(a) and (b). The initial active power consumption is also identical (Fig. 8(c)), while the LFT+OLTC initially needs extra reactive power to compensate the transformer leakage and line inductance, and exciting current as well, but ST is regulated to output zero reactive power at same time.

After the contingency happened, for LFT+OLTC both primary and secondary voltage step reduce to around 0.9pu while for ST only primary voltage tends to reduce to 0.9pu in transient, but quickly stabilizes in 0.95pu as the reactive power compensated. The OLTC increases the secondary voltage discretely but only achieves 0.95pu in the end, this is because the limited steps for the tap. On the contrary, the voltage in secondary is fixed. Consequently, the loading is fixed in ST delivered network while is reduced in LFT delivered network. Due to lack of STATCOM, the reactive power in LFT primary is reduced after contingency following the voltage reduction.

Fig. 9 is the LFT+OLTC power-voltage curve in this case study. The secondary line impedance is neglected in the operation analysis, so that the power-voltage curve for primary side and secondary side of LFT is identical. Initially, the operating point is A for both primary and secondary. After contingency, the operating point immediately moves to B in both sides and voltage drops to 0.9pu as shown in Fig. 8(a) and (b). Since the LFT+OLTC slowly increases the secondary voltage to 0.95pu, the secondary operating point moves from B to C, while, to balance the active power, the primary operating

point moves from B to D. Therefore, the active power recovers following to the secondary voltage increase, but the primary voltage has slightly reduction (Fig. 8(b)).

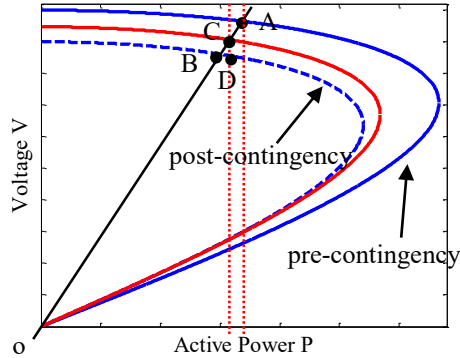


Fig. 9. LFT+OLTC Power-voltage curve in case study

Fig. 10 is the ST power-voltage curve in this case study. Similarly, the operating point is A for both primary and secondary at initial state. After contingency, due to the isolated voltages in primary and secondary, the secondary operating point keeps on A while the primary operating point tends to move to B transiently. However, because of the quick reactive power compensation, the primary voltage increases to 0.95pu (Fig. 8(b)) and its operating point stabilizes on C.

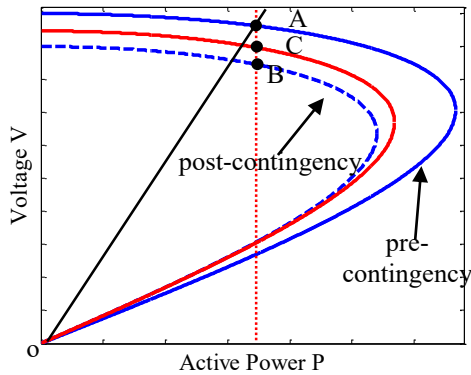


Fig. 10. ST Power-voltage curve in case study

In total, after contingency, ST keeps the secondary voltage as operating point A in Fig. 10 while LFT+OLTC behaves voltage reduction as operating point moving to C in Fig. 9; in secondary, ST helps support the voltage by reactive power compensation, as consequent, the voltage slightly reduces as operating point moving to C in Fig. 10. However, the voltage further drops when the OLTC increasing secondary voltage as operating point moving to D in Fig. 9. In this process, obviously, the system is more robust, and the voltage stability is enhanced in the ST delivered system.

VI. CONCLUSION

This paper mathematically analyses and compares the power delivery characteristic of smart transformer and low frequency transformer combed with STATCOM or load tap changer by means of the power-voltage curve. The inclusion of ST in the system helps break the electric distance between the load and generator, and possibly increase the maximum power delivery

(restricted by the smart transformer power capacity). The decoupled voltage in the MVAC and LVAC helps control the loading, and the decoupled reactive power in these two sides helps support the upper-stream network voltage. The case study validates that the smart transformer improves system voltage stability and fast load regulation.

ACKNOWLEDGMENT

This work is part of Energy Systems Integration Partnership Programme (ESIPP) Project funded by the Science Foundation Ireland (SFI) Strategic Partnership Programme Grant Number SFI/15/SPP/E3125, and is part of the European Research Council under the European Union's Seventh Framework Programme (FP/2007-2013)/ERC Grant Agreement 616344 HEART—the Highly Efficient And Reliable smart Transformer.

REFERENCES

- [1] M. Liserre, G. Buticchi, M. Andresen, G. Carne, L. Costa and Z. Zou, "The smart transformer: impact on the electric grid and technology challenges," *IEEE Ind. Electron. Magazine*, Jun. 2016.
- [2] Energy conversation program for commercial equipment (2007). Distribution transformers energy conversation standards, CFR Standard 431, Oct. 2007.
- [3] X. Gao, R. Zhu, G. De Carne and M. Liserre, "Comparison of voltage support services by means of STATCOM and smart transformer in medium voltage grid," *2018 13th IEEE Conference on Industrial Electronics and Applications (ICIEA)*, Wuhan, 2018, pp. 946-951.
- [4] X. Gao, G. De Carne, M. Liserre and C. Vournas, "Voltage control by means of smart transformer in medium voltage feeder with distribution generation," *2017 IEEE Manchester PowerTech*, Manchester, 2017.
- [5] J. Chen, C. Loughlin and T. Donnell, "Dynamic demand minimization using a smart transformer," *43rd Annual Conference of the IEEE Industrial Electronics Society (IECON)*, Beijing, China, Nov. 2017.
- [6] T. V. Cutsem and C. Vournas, "Voltage stability of electric power systems," *Power Electronics and Power Systems Series*. Kluwer Academic Publishers, 1998.
- [7] P. Kundur, "Power system stability and control," 978-0-07-035958-1, 1994.
- [8] F. Milano, *Power system modelling and scripting*, Springer, London, August 2010.
- [9] C. Wang, X. Yin, Z. Zhang and M. Wen, "A novel compensation technology of static synchronous compensator integrated with distribution transformer," *IEEE Trans. Power Del.*, vol. 28, no. 2, pp. 1032-1039, April 2013.
- [10] C. Ö. Gerçek and M. Ermis, "Elimination of coupling transformer core saturation in cascaded multilevel converter-based T-STATCOM systems," *IEEE Trans. Power Electron.*, vol. 29, no. 12, pp. 6796-6809, Dec. 2014.
- [11] H. Xie, L. Angquist, and H. Nee, "Comparison of voltage and flux modulation schemes of statcome regarding transformer saturation during fault recovery," *IEEE Trans. Power Sys.*, vol. 23, no. 4, Nov. 2008.
- [12] S. M. Abd-Elazim and E. S. Ali, "Optimal location of STATCOM in multimachine power system for increasing loadability by Cuckoo Search algorithm," *International Journal of Electric Power & Energy Systems*, Vol. 80, pp. 240-251, Sep. 2016.
- [13] J. Chen, R. Zhu, M. Liserre and T. O'Donnell, "Neutral current reduction control for smart transformer under the imbalanced load in distribution system," *2018 13th IEEE Conference on Ind. Electron. and Applications (ICIEA)*, Wuhan, 2018, pp. 2381-2386.
- [14] J. Chen, C. O'Loughlin and T. O'Donnell, "Dynamic demand minimization using a smart transformer," *IECON 2017-43rd Annual Conference of the IEEE Ind. Electron. Society*, Beijing, 2017, pp. 4253-4259.
- [15] J. Chen, R. Zhu, M. Liserre and T. O'Donnell, "Smart transformer for the provision of coordinated voltage and frequency support in the grid," *IECON 2018-44th Annual Conference of the IEEE Ind. Electron. Society*, Washington, DC, USA, 2018.